The Spectromicroscopy Beamlines at Elettra: Recent Achievements

S. Heun

Elettra, Sincrotrone Trieste, Basovizza, 34012 Trieste, Italy

electrons
photons
ions
atoms

emission of
particles

SAMPLE

- UHV compatibility
- escape depth / surface sensitivity
- (non-) destructive method
- optics / lenses available
- signal-to-background ratio
- cross-section for excitation

AUGER LINES

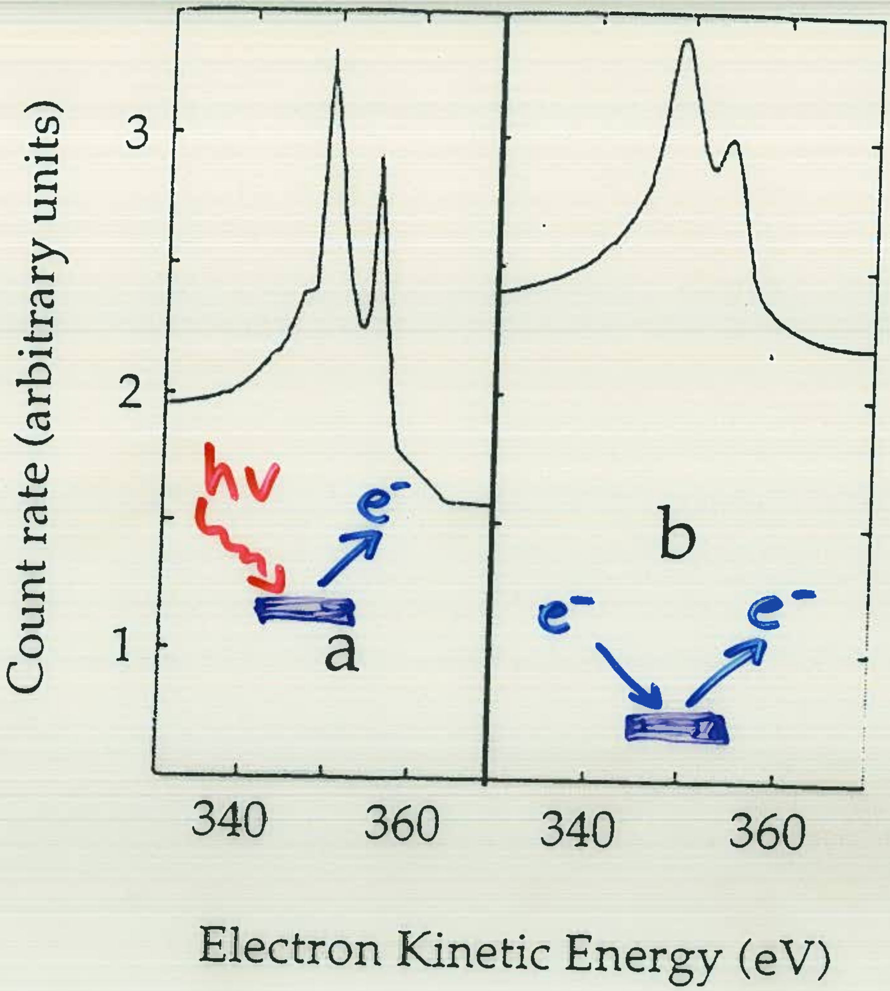

$\Delta E \approx$ several eV

Fig. 2. Comparison of the Ag$M_{4.5}VV$ Auger peaks obtained with (a) MgK_α radiation (data from Ref. 16) and (b) 3-keV electron bombardment (data from Ref. 17).

CORE LEVEL PEAKS

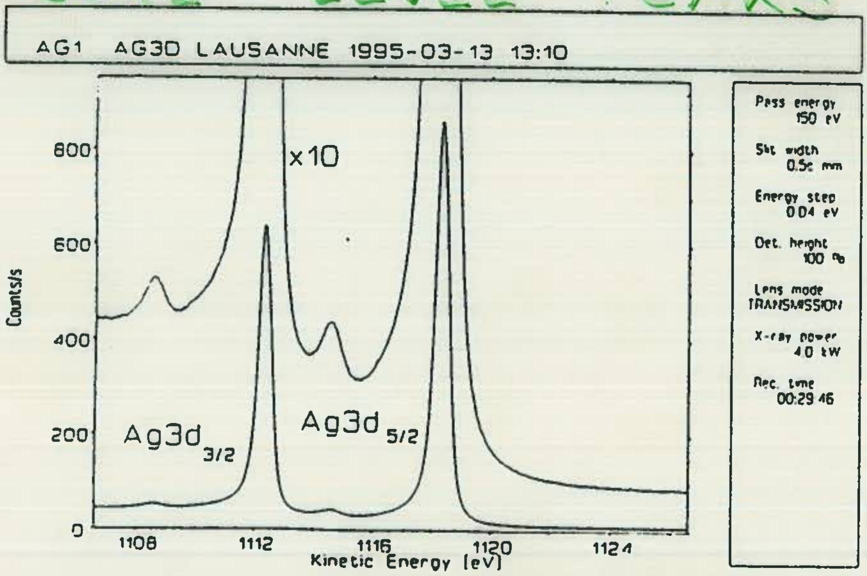

$\Delta E < 1$ eV

Fig. 3. Ag-3d$_{3/2,5/2}$ peaks, excited with AlK_α radiation ($h\nu = 1486.6$ eV). The characteristic photoelectron peaks are much narrower than Auger electron peaks as it is clearly seen by a comparison with the $M_{4.5}VV$ Auger peaks in Fig. 2.

SR – PHOTOELECTRON SPECTROSCOPY

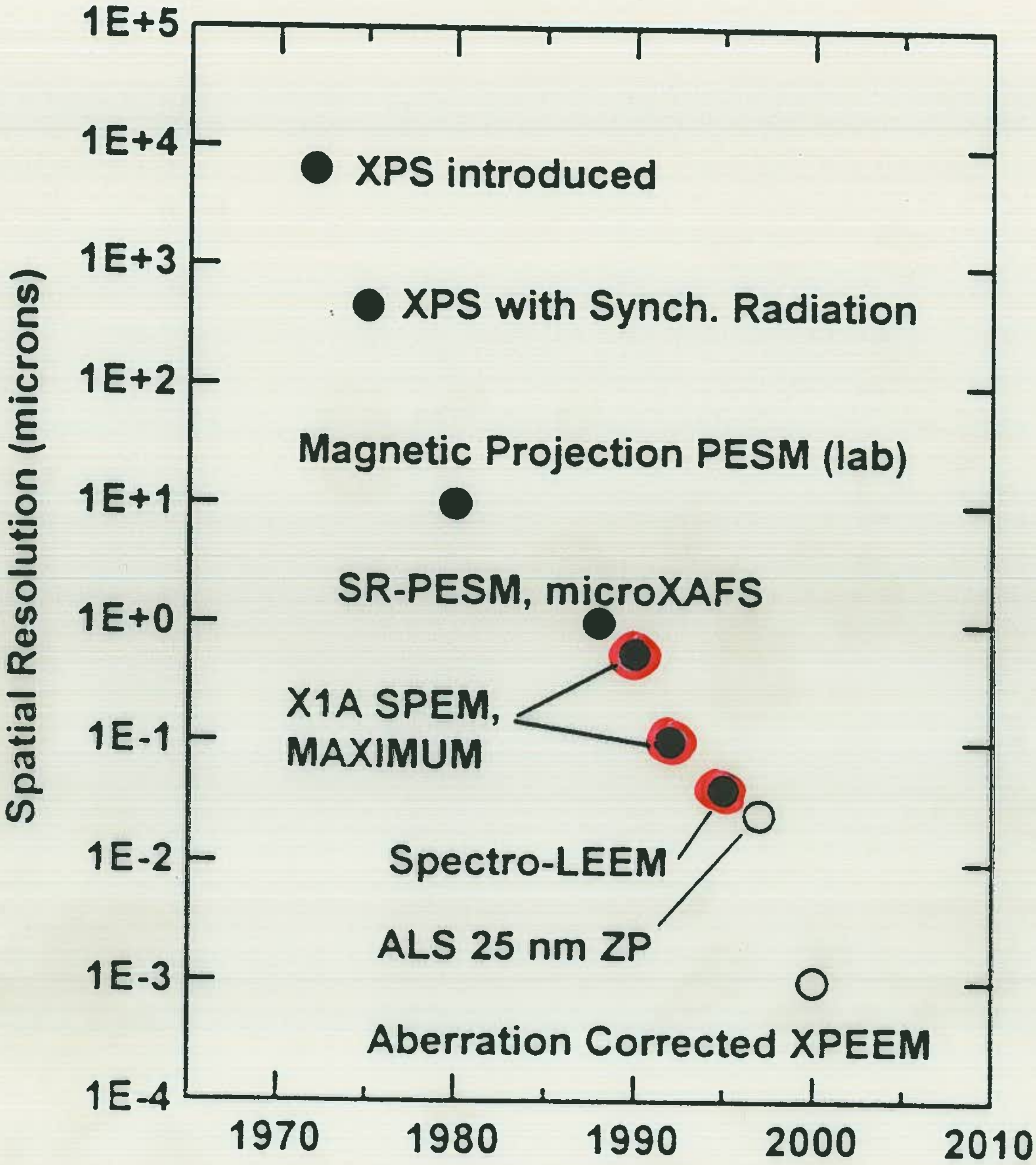

Fig. 11. Historical development of spectromicroscopy, including results from both photoelectron and X-ray absorption instruments. The remarkable improvements in spatial resolution are evident. The open circles are projects under construction, a zoneplate microscope at the ALS, and an aberration corrected electron imaging microscope proposed for Bessy II.

Spectromicroscopy – microspectroscopy

Scanning mode – imaging mode

scanning spectromicroscopes:

- Fresnel zone plates (100 nm) (100 meV)
- Schwarzschild objective (200 nm)

⊕ any sample
⊕ combination with standard analyzer
⊖ mechanical movement of sample
⊖ very high photon density on sample

imaging mode:

- XPEEM (20 nm) (500 meV)

⊕ best time resolution (1 ms)
⊕ radiation source not sharply focused
⊖ need for flat samples

$$\text{brilliance} = \frac{\text{photons}}{\text{time} \times \text{bandwidth} \times \text{source size} \times \text{source solid angle}}$$

S ΔD

$$S\Delta D = \text{constant} = S'\Delta D'$$

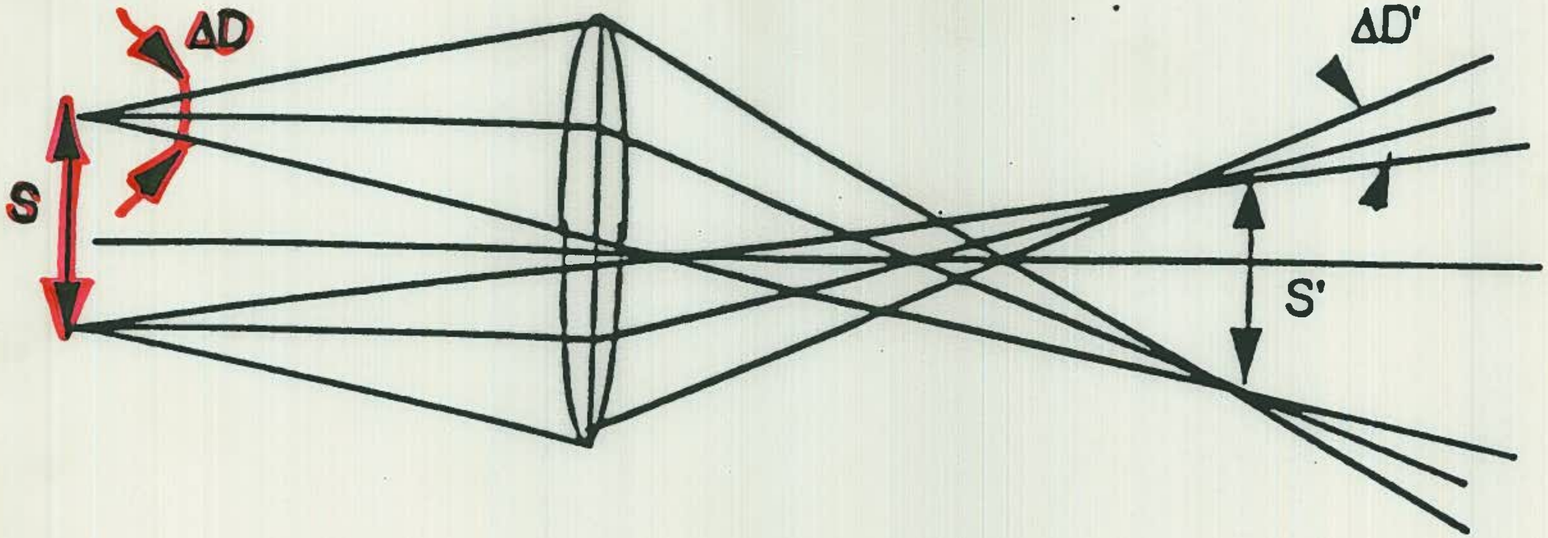

Fig. 1. The Liouville theorem applied to optics states that for an optical system the product of beam size × beam divergence is constant along the optical path.

THIRD GENERATION LIGHT SOURCE

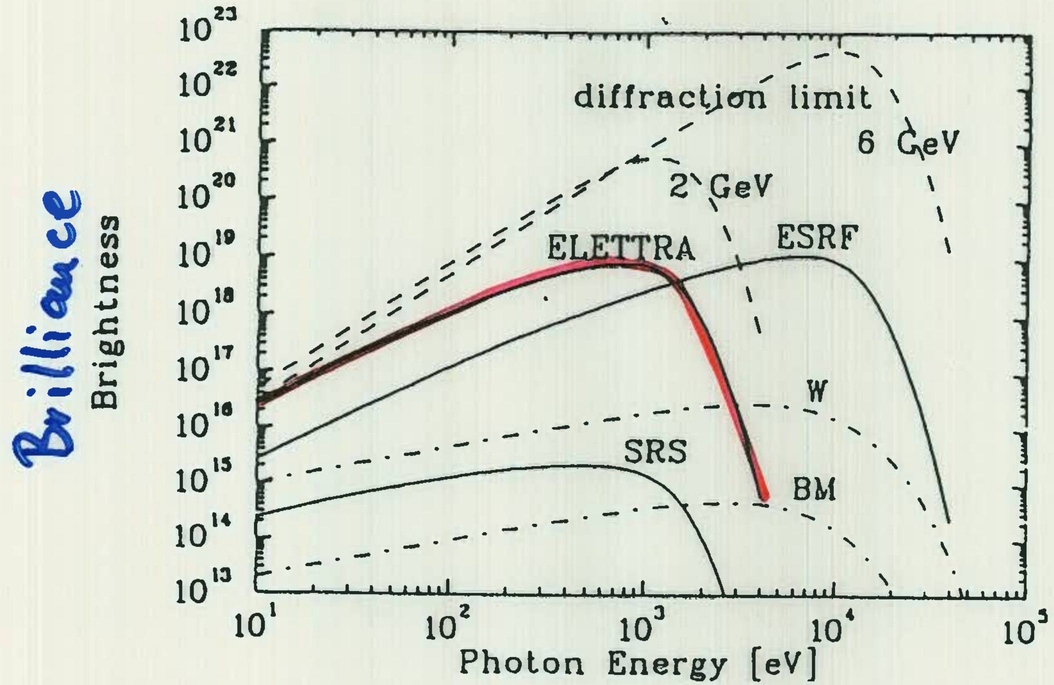

Fig. 2. Synchrotron radiation brightness (photons/s/mm^2/mrad^2/0.1%bandwidth) for various rings. Beam current = 200 mA. Undulator length = 1 m (SRS), 4.5 m (ELETTRA), 1.6 m (ESRF), 5 m (diffraction limit); undulator gap = 20 mm. The brightness of a bending magnet (BM) and multipole wiggler (W) source in ELETTRA are also shown.

PATH DIFFERENCE

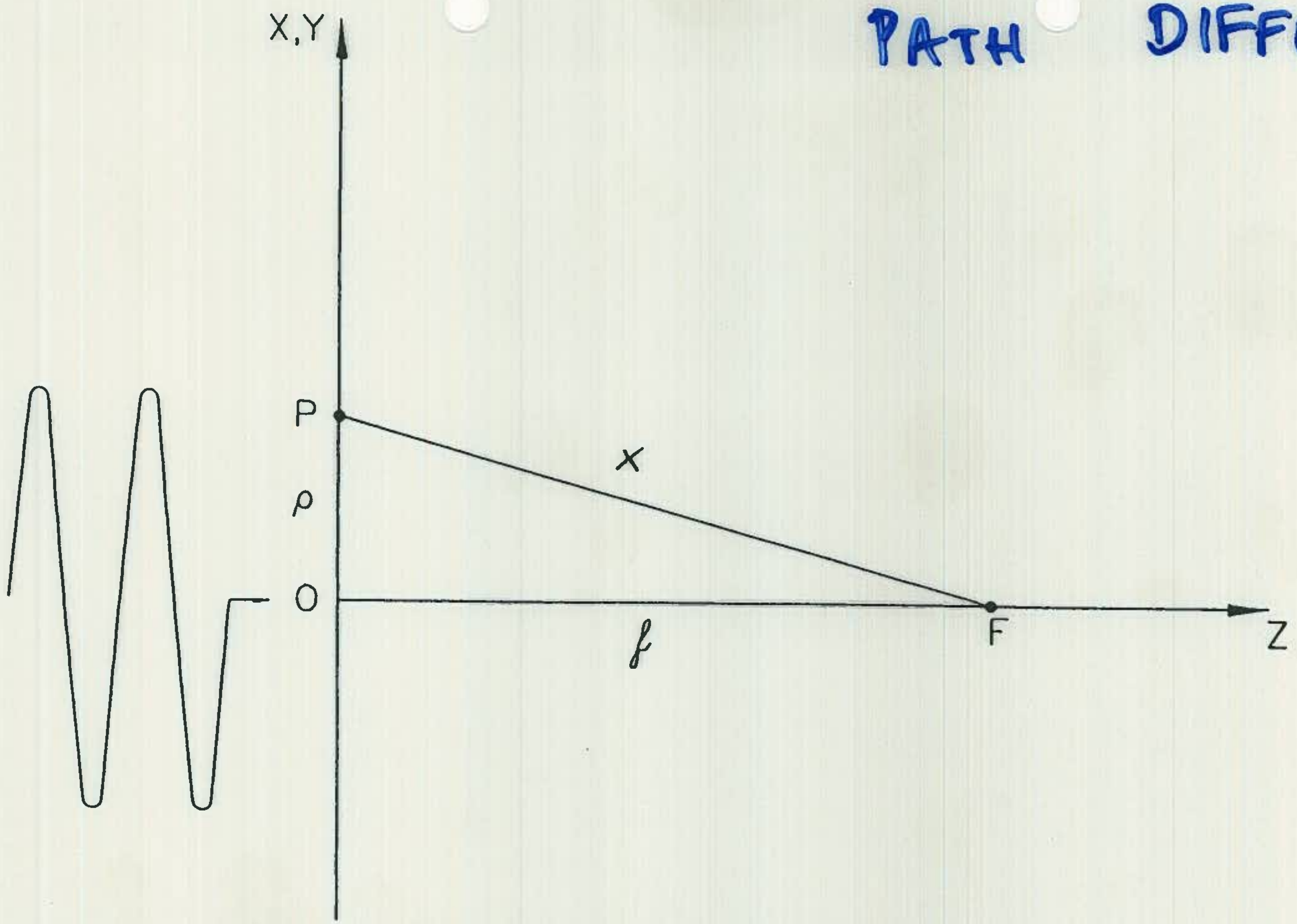

Fig. 5. The spherical waves emitted from points O and P of a plane wave front have an interference condition at point F which depends on the path difference PF - OF ≈ $\rho^2/2f$.

$$\boxed{\Delta = \frac{\rho^2}{2f}}$$

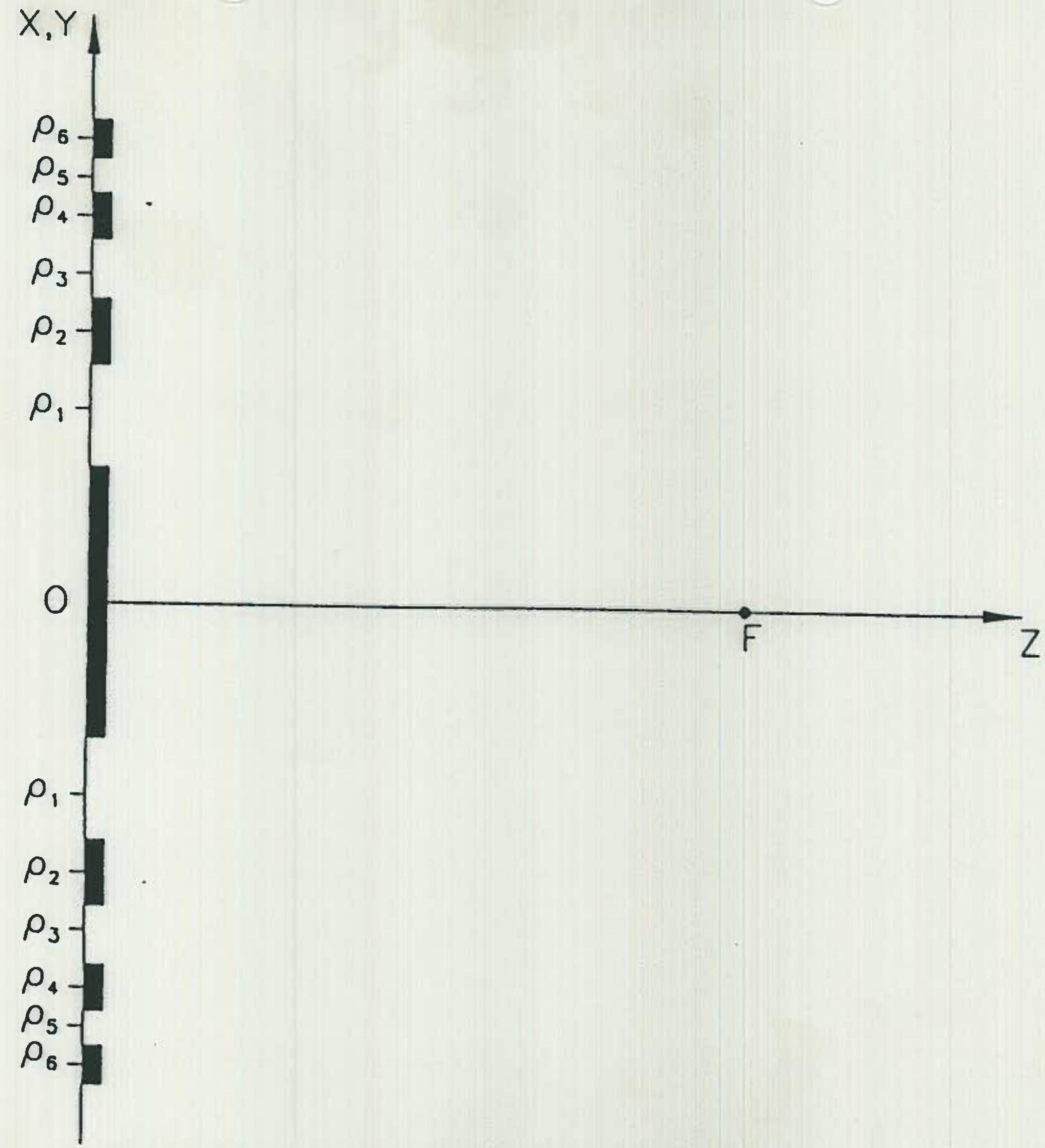

Fig. 6. A Fresnel zone plate is a grating made of rings, named Fresnel zones, with radii ρ_n. The rings are absorbing for n even and transparent for n odd (or viceversa).

FRESNEL ZONE PLATES

$$\Delta = \frac{\rho^2}{2f}$$

$$\rho_n = \sqrt{n \lambda f}$$

Fresnel zones

Fig. 3. Front view of a Fresnel zone plate.

HUYGENS-FRESNEL PRINCIPLE

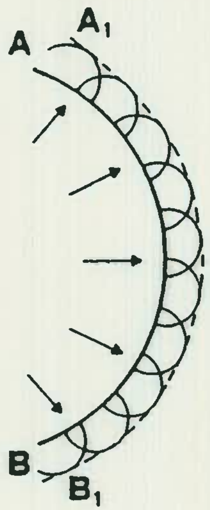

Fig. 4. Huygens-Fresnel principle: each point of the wave front AB emits a spherical wave at the time t. The wave front A_1B_1 is formed by the superposition of such spherical waves at the time $t+\Delta t$.

MULTPLE FOCI :

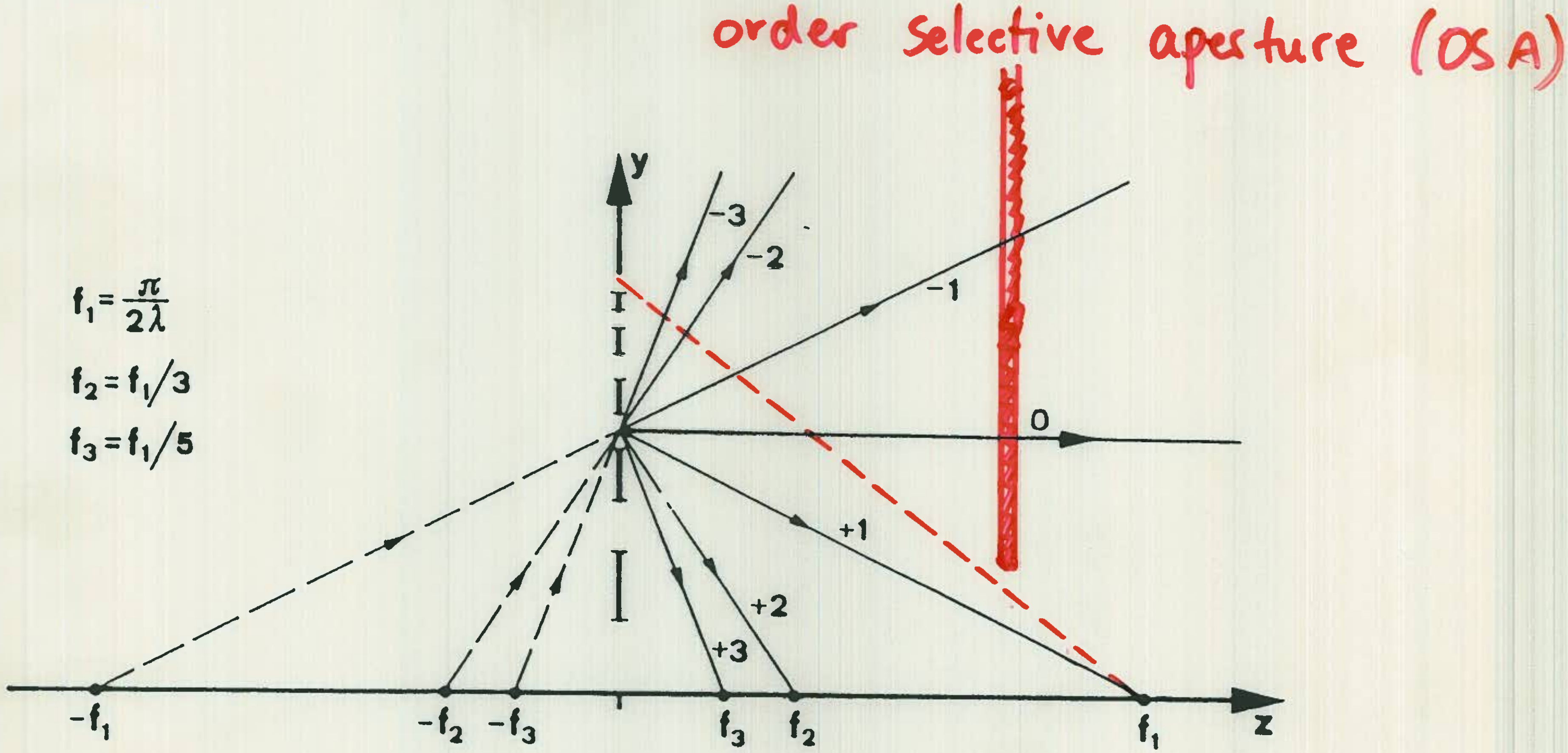

Fig. 7. A zone plate has a number of foci corresponding to the different diffraction orders. The zero order corresponds to rays which pass through the transparent rings of the zone plate without changing their direction, as foreseen by geometrical optics. The positive (negative) orders give rise to real (virtual) images.

zone plate efficiency (1st order): $1/\pi^2 \approx 10\%$

MINIMUM SPOT SIZE δ

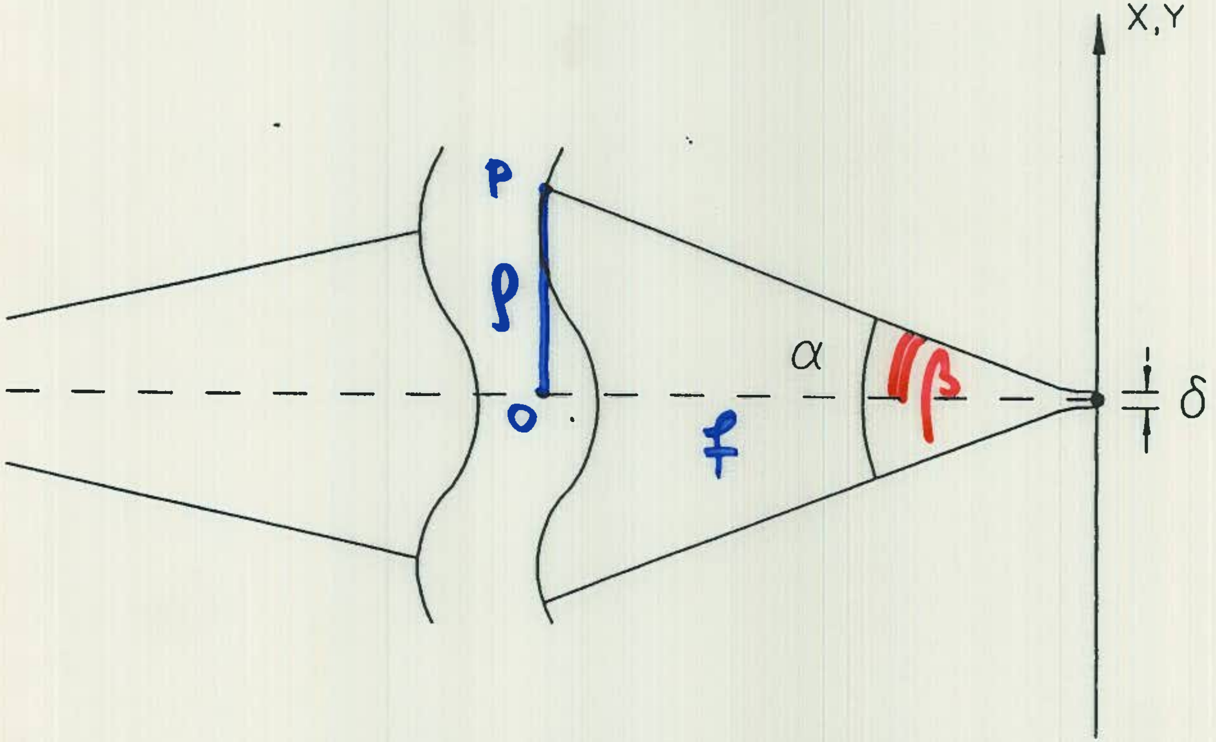

Fig. 8. The minimum spot size δ obtainable with an optical system is limited by diffraction. The "diffraction limit" δ is inversely proportional to the "numerical aperture" NA, which is the sine of the half angle α/2 of the light cone which is focused on the spot.

$$\delta = \frac{\lambda}{2 \sin \beta} = \frac{\lambda}{2\ NA}$$

NA: numerical aperture

$NA = \rho_m / f$

$$\delta = \frac{\lambda}{2 \sin \beta} \qquad \sin \beta = \frac{\rho_m}{f}$$

$$\rho_m = \sqrt{m \lambda f}$$

$$= \frac{1}{2} \sqrt{\frac{f\lambda}{m}}$$

Thickness of outermost zone:

$$\Delta \rho_m = \rho_{m+1} - \rho_m$$

$$= \frac{1}{2} \sqrt{\frac{f\lambda}{m}} = \delta$$

zone plate ∅ $D = 2\rho_m = 2\sqrt{m\lambda f}$

$\Delta\rho_m = \frac{1}{2}\sqrt{\frac{\lambda f}{m}}$

$\rightsquigarrow \; D \times \Delta\rho_m = \lambda f$

$\Leftrightarrow \; f = \frac{D \times \Delta\rho_m}{\lambda}$

D : 100 µm

$\Delta\rho_m$: 100 nm

λ : 2.5 nm (500 eV)

$$\boxed{f = 4\,mm}$$

→ m = 250 rings

Photon focusing elements

Diffractive elements: Fresnel zone plates (T)

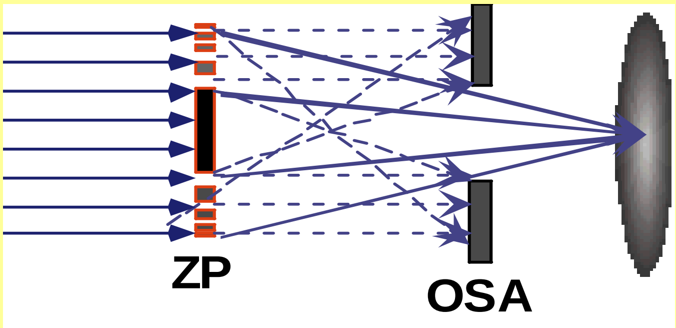

200-12000 eV

R = 1.22∂r_n (300 Å)

f =Dδr_nE;

efficiency

(% diffracted photons)

Bragg-Fresnel optics (R)

Reflective elements: mirrors:

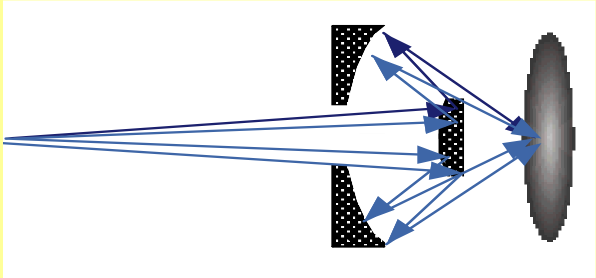

normal incidence spherical mirrors

Schwarzschild objectives

< 160 eV, R-90 nm

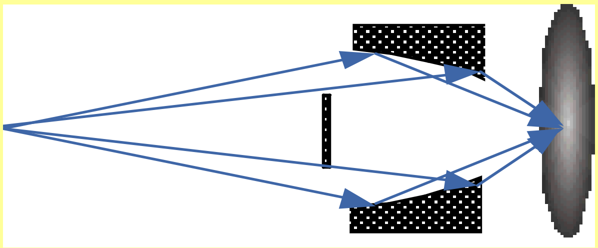

grazing incidence (bendable mirrors)

Ellipsoidal mirror

R< 1 µm,
full energy tunability

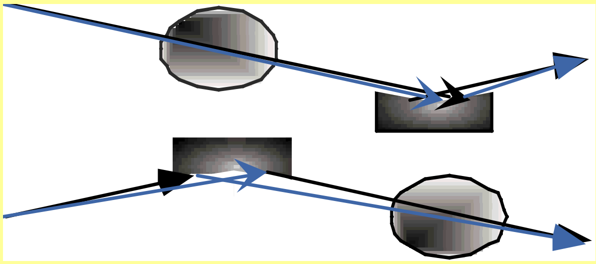

Kirkpatrick-Baez arrangement

IMAGING AND MICROSPECTROSCOPY

IMAGE CONTRAST
- Concentration variations.
- Chemical state variations.
- Topographic features.

SPECTROSCOPY
- PE core level intensities.
- PE core level shifts.
- VB: electronic structure.

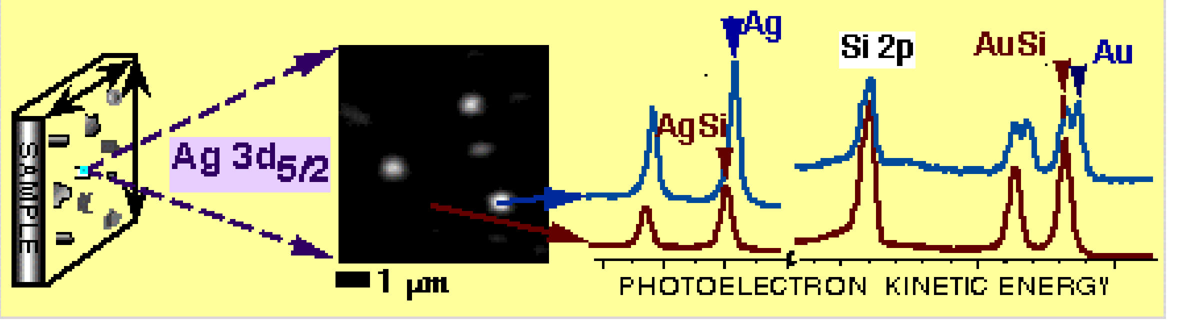

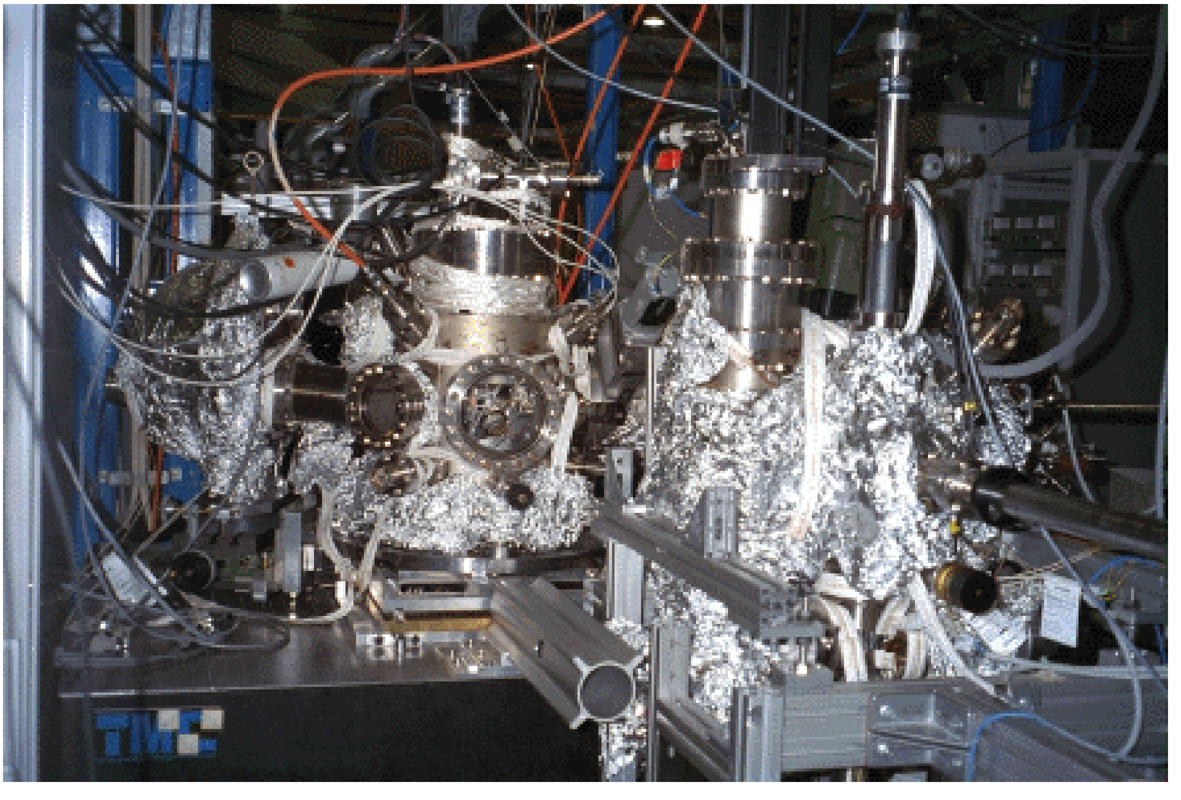

Aproaches to SR-XPS-microscopy

Photon optics to demagnify the beam:
scanning instruments

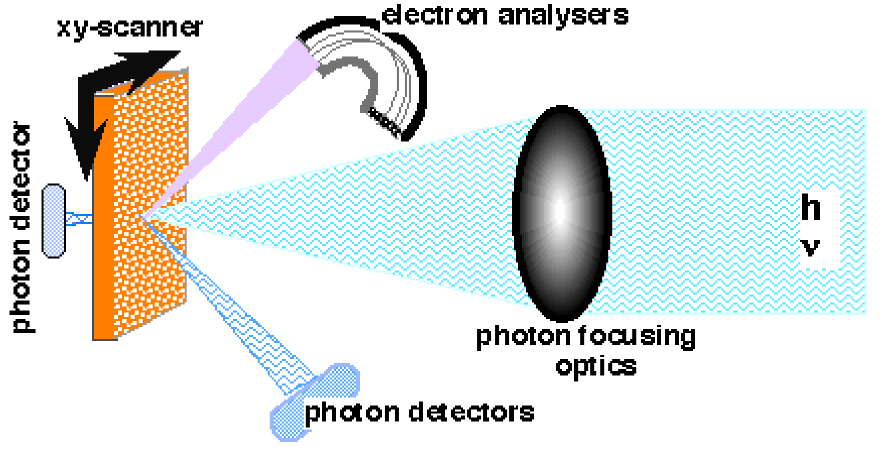

1. Whole power of XPS in a small spot spectrscopy mode;
2. Flexibility for adding different detectors;
3. Limited applications for fast dynamic processes;
4. Lower resolution than imaging instruments.

Electrostatic optics to magnify the irradiated area:
imaging instruments

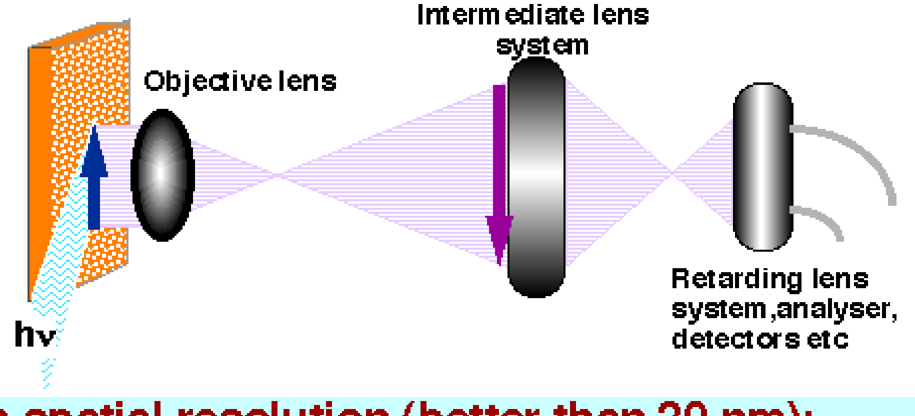

1. High spatial resolution (better than 20 nm);
2. Multi-method instrument: XPEEM/PED & LEEM/LEED;
3. Excellent tool for monitoring dynamic processes;
4. More difficult to operate and sensitive to rough surfaces.

Ni/Si Interface: imaging of Si 2p chemical shifts

⌘ 16-channel detection with high spectral resolution

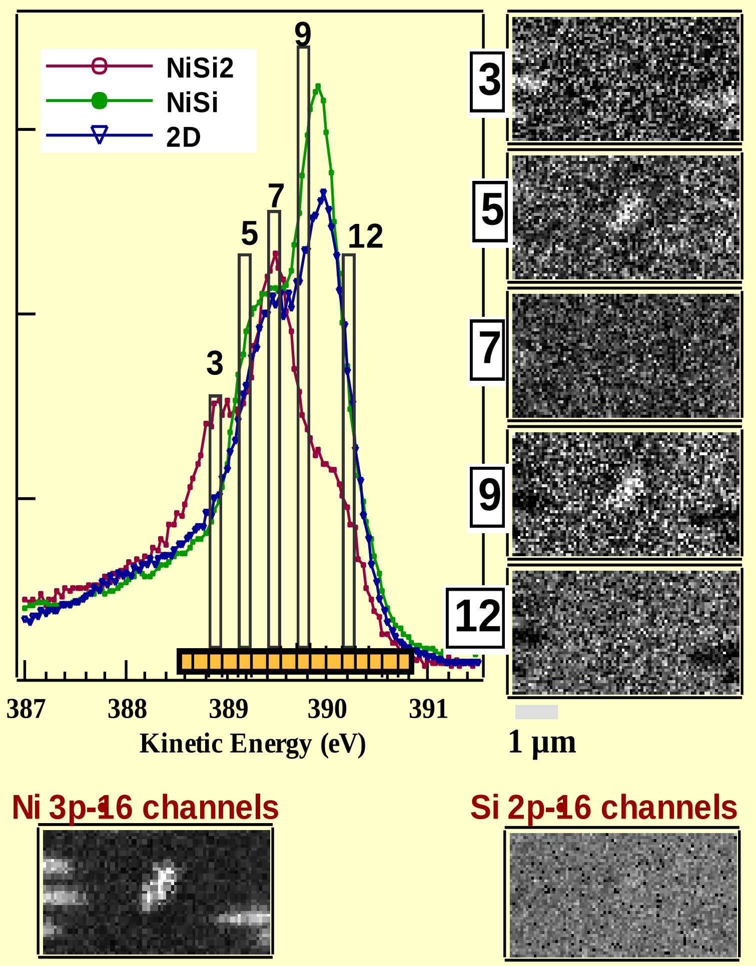

ESCAMicroscopy group: ELETTRA

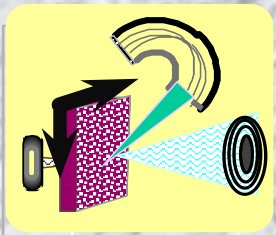

Some other microscopes

- X-ray microscopes:
- SR-STXM combined with NEXAFS - Resolution < 50nm. Bulk sensitive, does not require UHV. Needs thin samples. O, C, N and L edges. Biological samples, polymers, magnetic materials etc.
- SR-FA& XANES microprobe - Resolution ~ 1-2 µm. Bulk sensitive, does not require UHV. Excellent instrument for detecting precipitates, inclusions, impurities in various materials.
- Commercial XPS - Resolution ≥ 10 µm. Less surface sensitive.
- Electron microscopes:
- Commercial SAM - Resolution better than 100 nm. Surface sensitive, but more radiation damage and limited chemical sensitivity.
- Commercial SEM-FA, TEM-EELS - Resolution better than 10 nm. Bulk sensitive, more radiation damage .

Continuous and interrupted interfaces

- Simultaneous investigation of the phases inside, outside and at the forefront of the confined film: essential step to understanding the evolution of non-uniform multi-element interfaces.
- Competing local processes controlling the evolution of the interfaces:
  - Local interactions: (i) displacement; (ii) alloying; (iii) 'new' compound formation;..
  - Mass transport: (i) surface diffusion due to thermal and/or electromigration; (ii) incorporation in and/or re-deposition from the 3D islands...

Au patch on √3Ag/Si

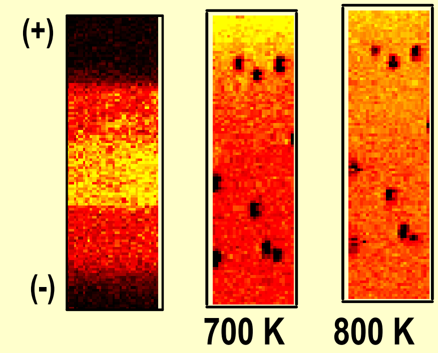

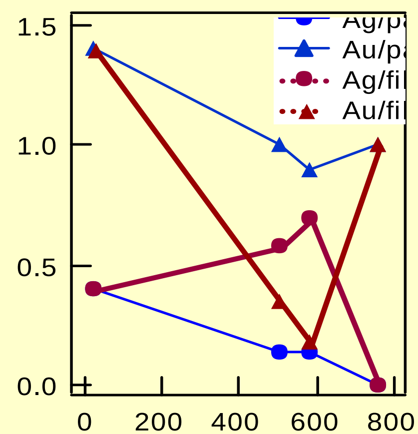

ARTEFACTS IN SPECTROMICROSCOPY

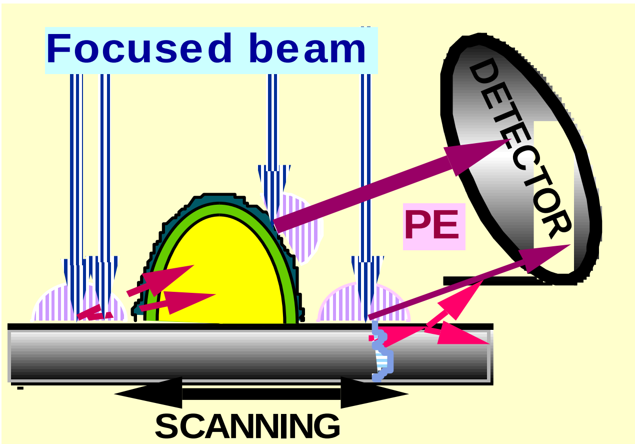

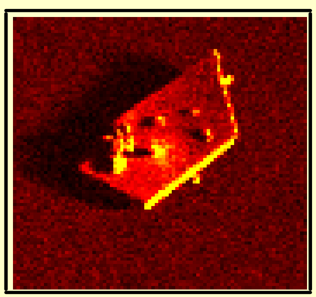

- **Topographic artefacts:** the curvature of the surface results in anisotropy of PE angular distribution & shadowing.
- **Diffraction, back scattering of the outgoing photoelectrons:** variations in the sub-surface substrate structure and composition.
- **Deceleration and deflection of outgoing photoelectrons, time-dependent charging**: local electrostatic field due to charging of samples with low conductivity.
- **Photon-induced processes.**

XPS Microscopy Artefacts

Photon-induced processes:

* oxide reduction;

* C deposition etc.

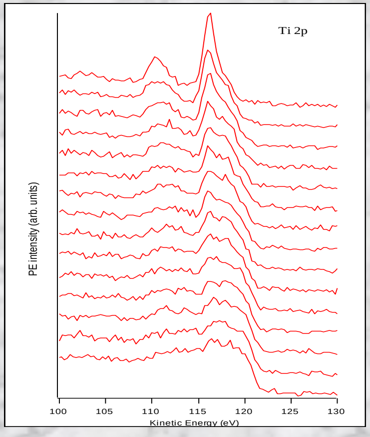

- Local Charging

10^9 ph/s ~ 10^8 atoms in ~ 1000 Å depth

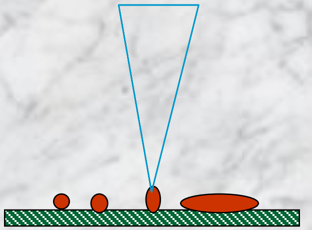

~ 10^7 atoms ionized

τ: 0 - 10^4 sec;

I_{ph} = 50-500 pA);

ΔUmeas. up to 250 V

MoOx on Al_2O_3: Mo 3d maps

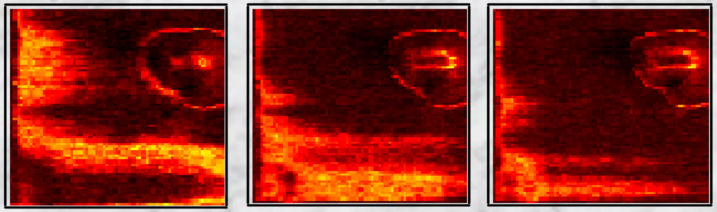

Time: 0 min 2 min 4 min

Band-bending changes across the transition regions of a p-n junction on a silicon device

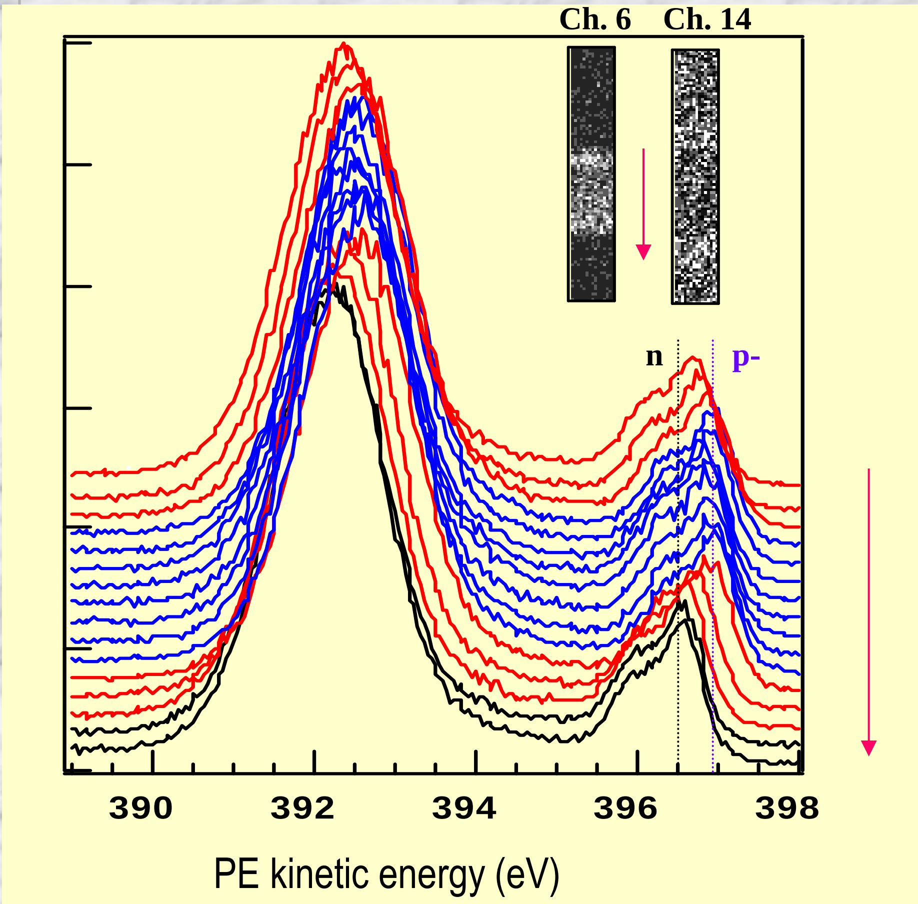

- Lateral p-n diode structure: p-stripe of a few microns fabricated by ion implantation of B through a mask of SiO_2 into n-doped Si(100).
- Contrast determined by the variations in the Fermi level pinning.
- The transition region was measured to expand up to 2 µm.

R. Phaneuf (UM-US) &ESCAMicrocopy

Beamline and scanning microscope layout

- Why do we need high brightness for microscopy?
  Atoms in 1 mm^2 - ~ 10^{13},   in 0.01 μm^2 ~ 10^5.
- Flux density in a 0.01 μm^2 spot should be > 10^8 ph/sec.

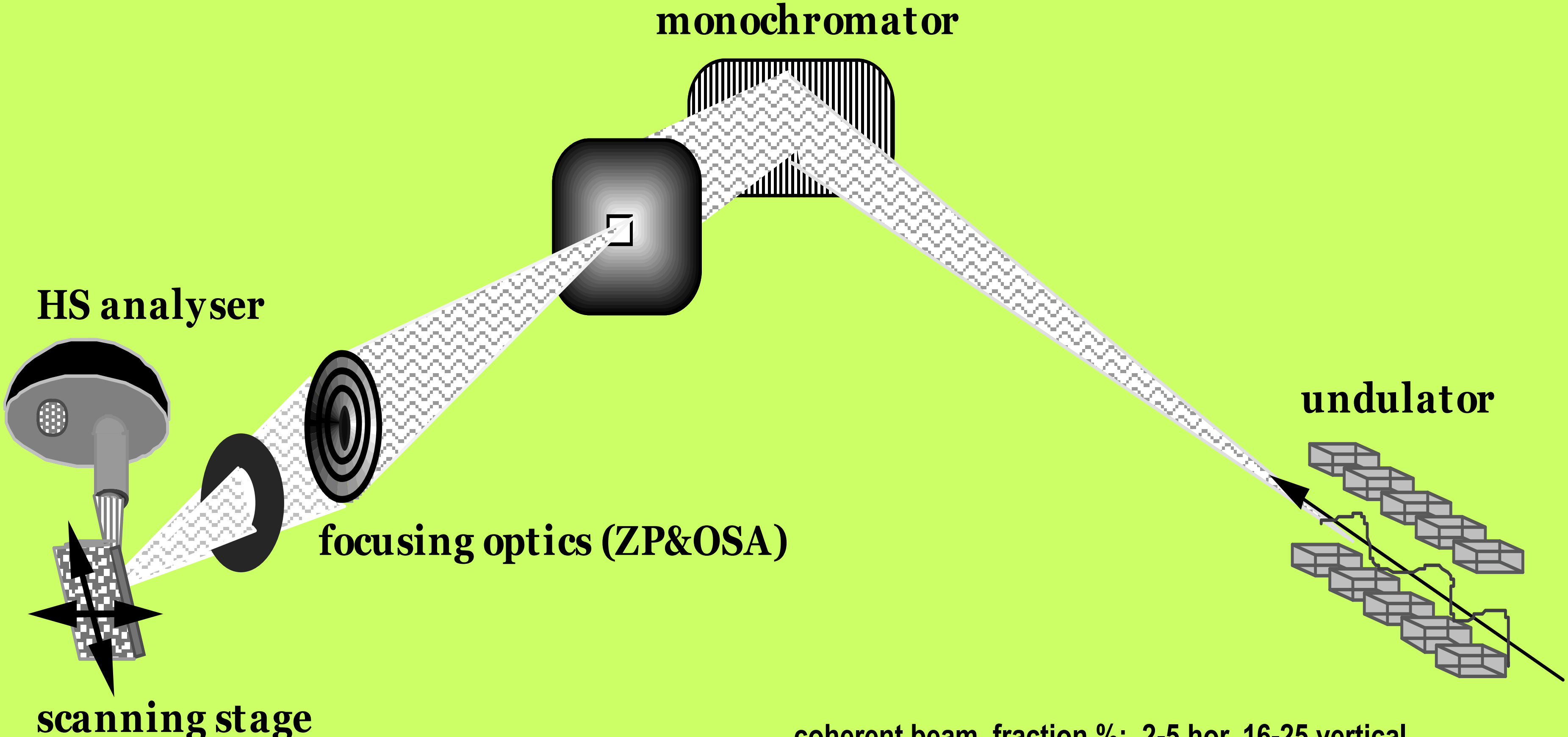

coherent beam fraction %: 2-5 hor, 16-25 vertical

Spatial Resolution of SPEM using 60 nm/200 µm Zone Plate fabricated in CXRO-Berkeley (Dr. E. Anderson)

AFM image

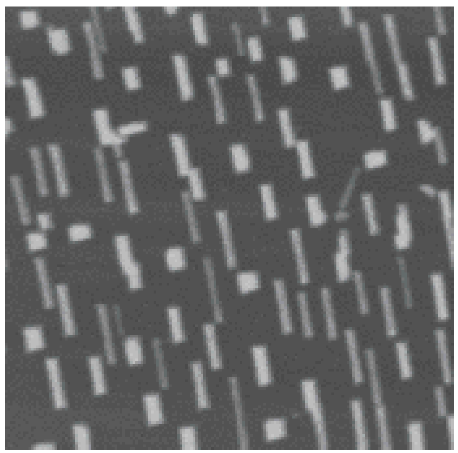

Fe 3p image

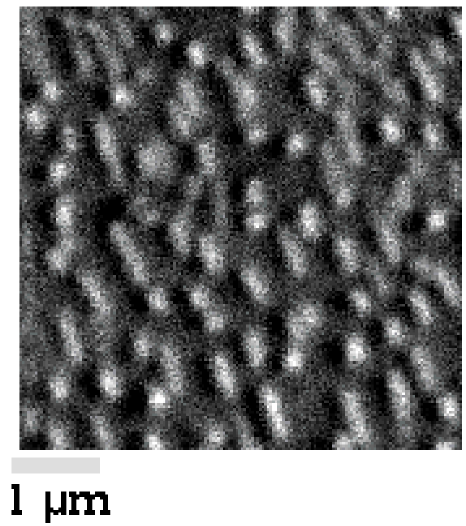

AFM and SPEM Images of assembled directionally grown $SmFe_2$ Films on a Mo Buffer, fabricated by pulsed laser deposition
(Project of Dr. J. Vogel at al, Louis Heel Lab-Grenoble, Feb. 99)

Maya Kiskinova:

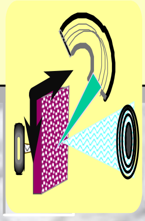

ologically complex semiconductor interfaces: gap in microcharacterization of lateral variations in the surface composition and electronic structure

- 2D and 3D micro-phases: formation stages and evolution;
- Mass transport at microscopic scales; 3D, 2D phases & confined films;
- Local chemical interactions, intermixing, segregation etc.

- SEM/FA: superior spatial resolution, no surface sensitivity;
- RHEED-TRAXS, SAM: inferior chemical information.

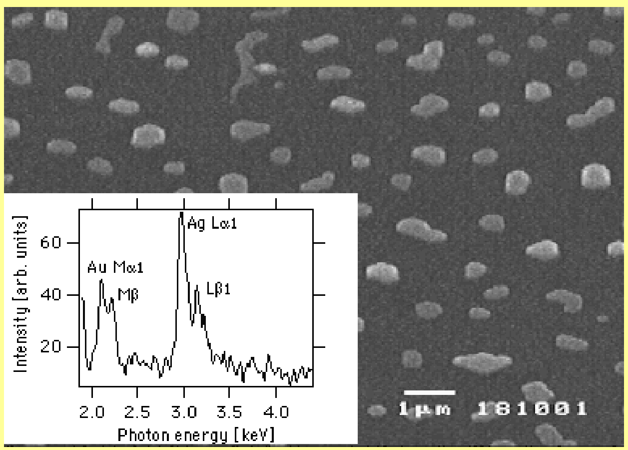

- SR-XPS microscopy: spatial resolution < 1000 Å, combined with high spectral resolution and surface sensitivity.

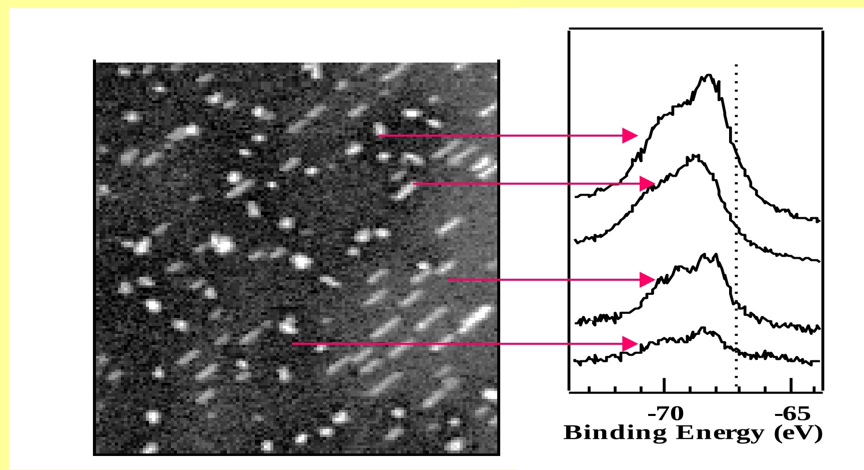

SCHWARZSCHILD OBJECTIVE

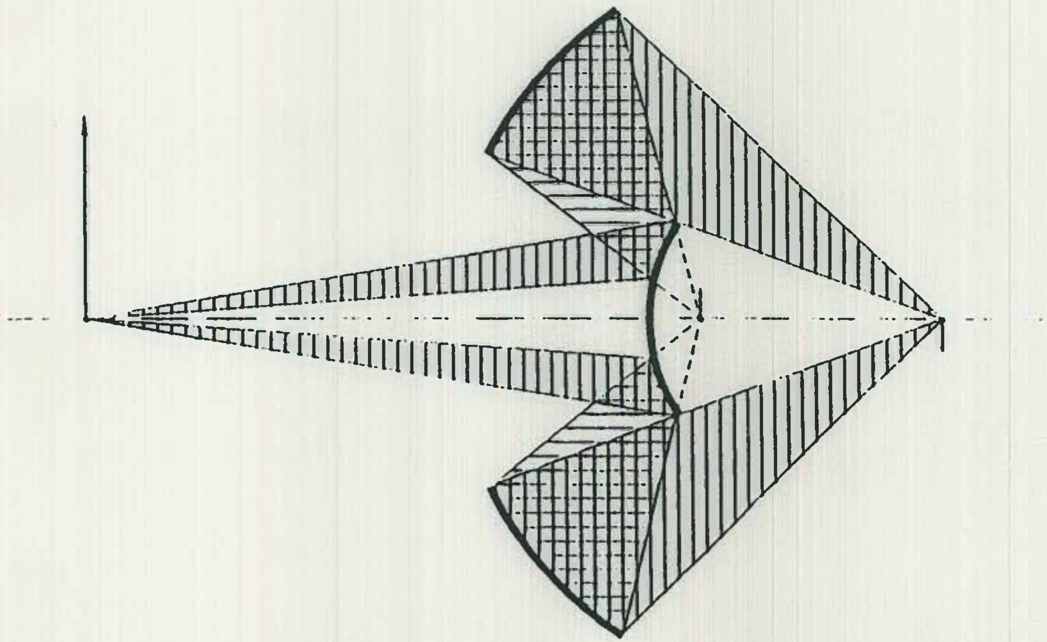

Fig. 9. Cross sectional view of a demagnifying Schwarzschild objective. The shaded areas indicate the rays that pass through the clear aperture of the system.

Light $\perp$ Mirrors

REFLECTIVITY OF GOLD

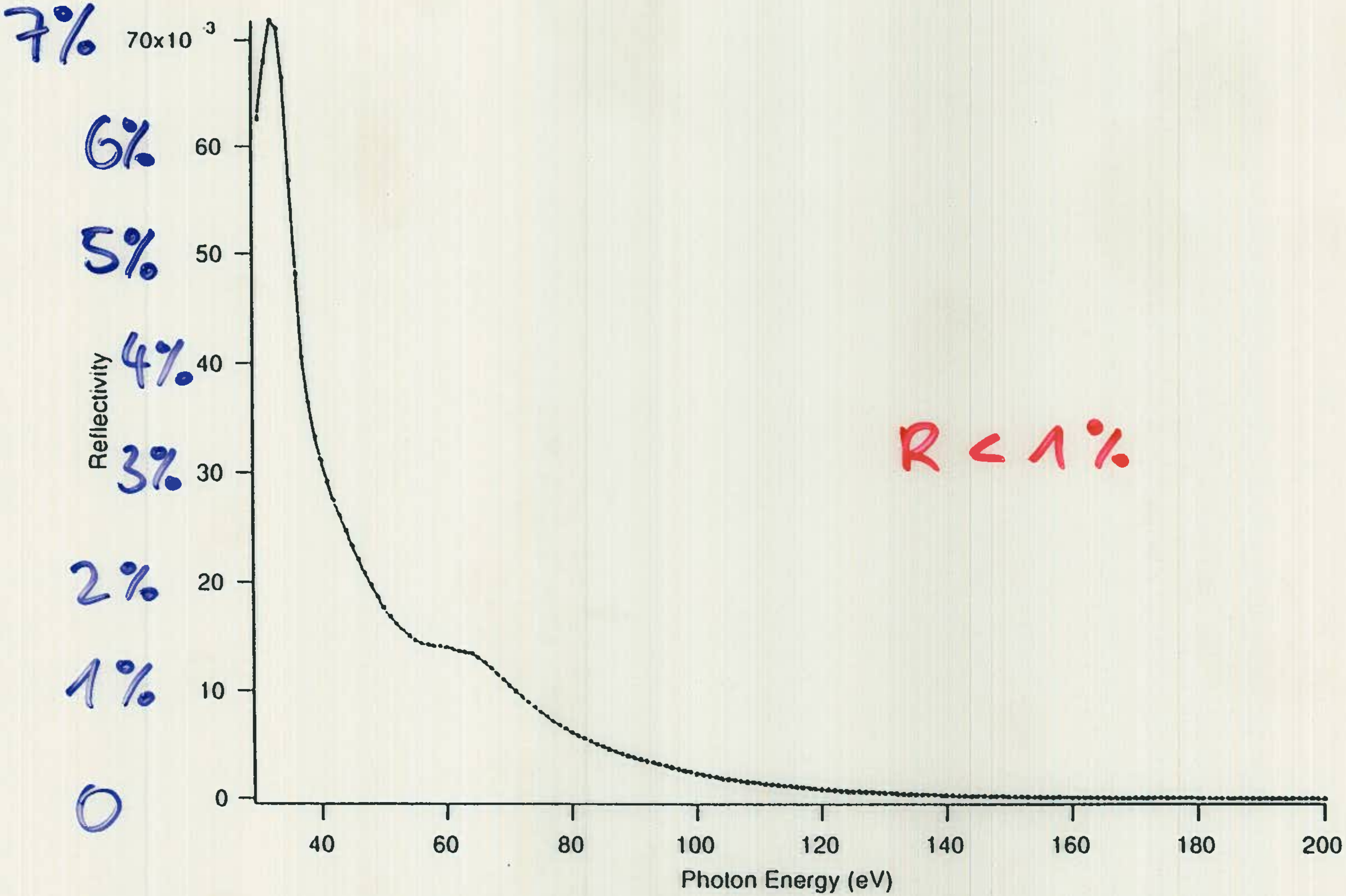

Fig. 10. Reflectivity of gold at normal incidence in the energy range 30-200 eV.

MULTILAYER COATING

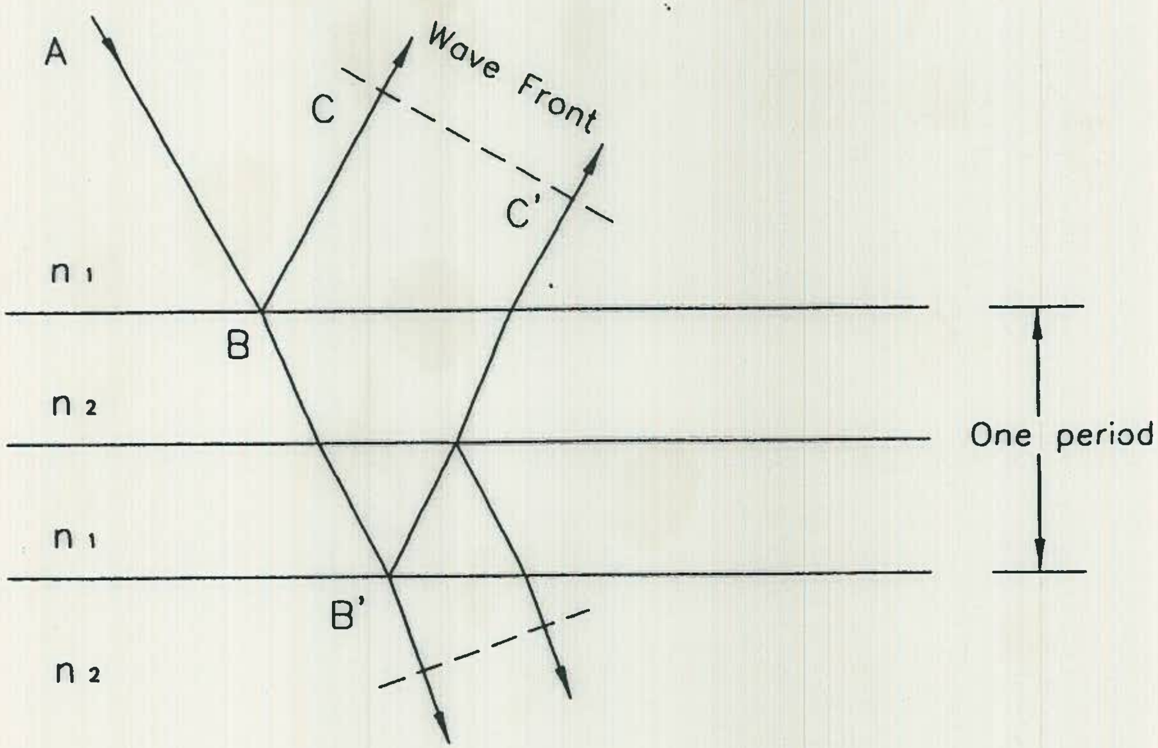

d

enhanced reflectivi

$\lambda = 2d$

Fig. 11. Working principle of a multilayer coating. The thickness of the period is chosen in such a way that the difference in optical path lengths ABC and AB'C' is one full wavelength (or multiple thereof), producing constructive interference at the reflected wave-plane.

$R \approx 50\%$

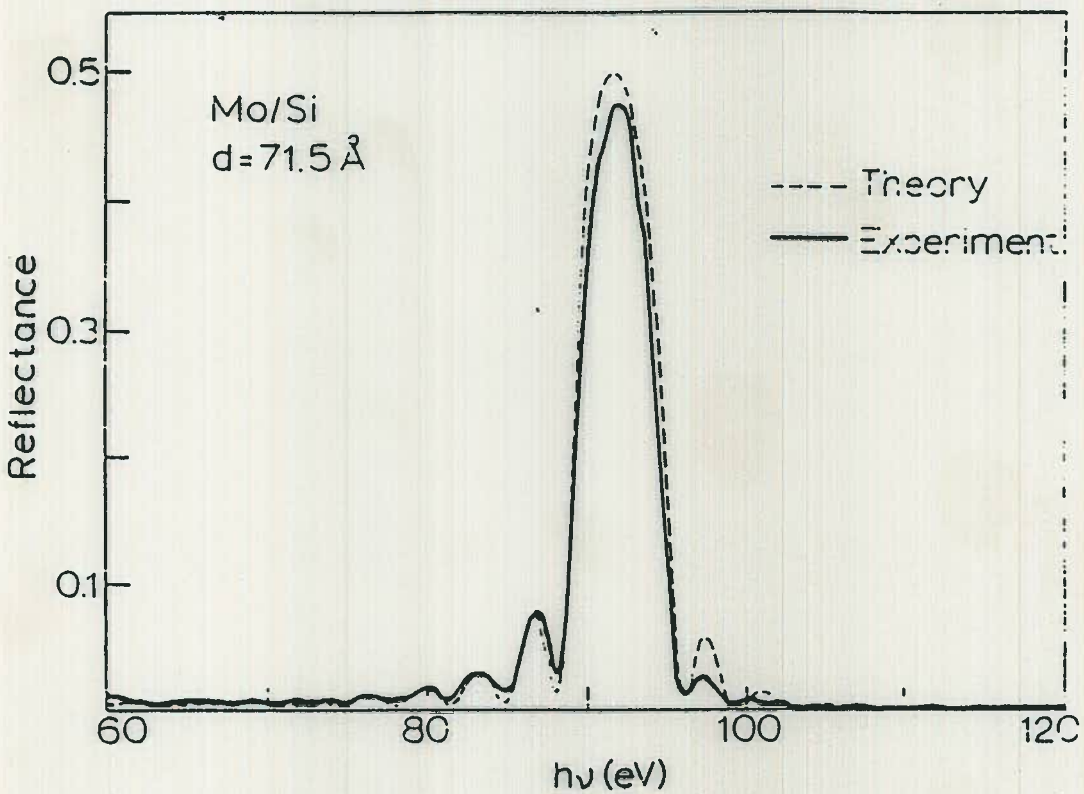

Fig. 12. Test of a 23-period Mo/Si multilayer coating with a period of 71.5 Å, deposited at the Berkeley Center for X-ray Optics.

$d = 71.5\,\text{Å} \rightarrow \lambda = 14.3\,\text{nm} \rightarrow E = 87\,\text{eV}$

$E = 500\,\text{eV} \rightarrow \lambda = 2.5\,\text{nm} \rightarrow d = 12.5\,\text{Å}$

Spectromicroscopy Beamline

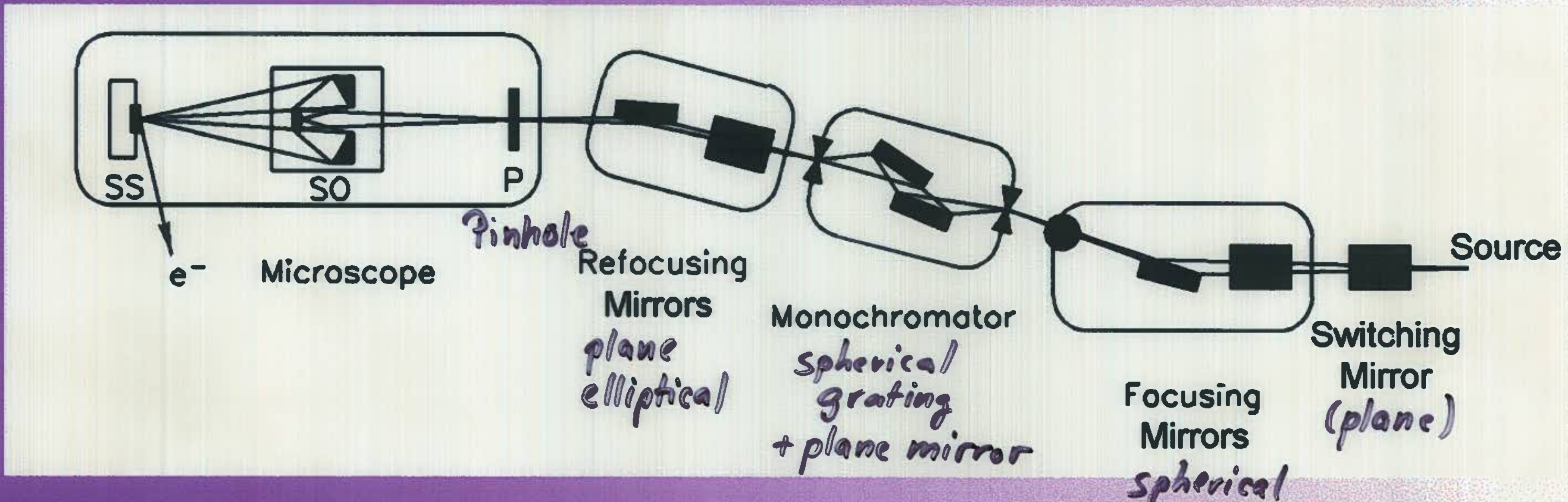

Monochromator resolving power: 2000

Photon Flux through 5 μm pinhole > 1 x 10^{12} photons / sec

F. Barbo, M. Bertolo, A. Bianco, G. Cautero, S. Fontana, T. K. Johal, S. La Rosa, G. Margaritondo, and K. Kaznacheyev, Rev. Sci. Instrum. 71 (2000) 5.

Schwarzschild Microscope

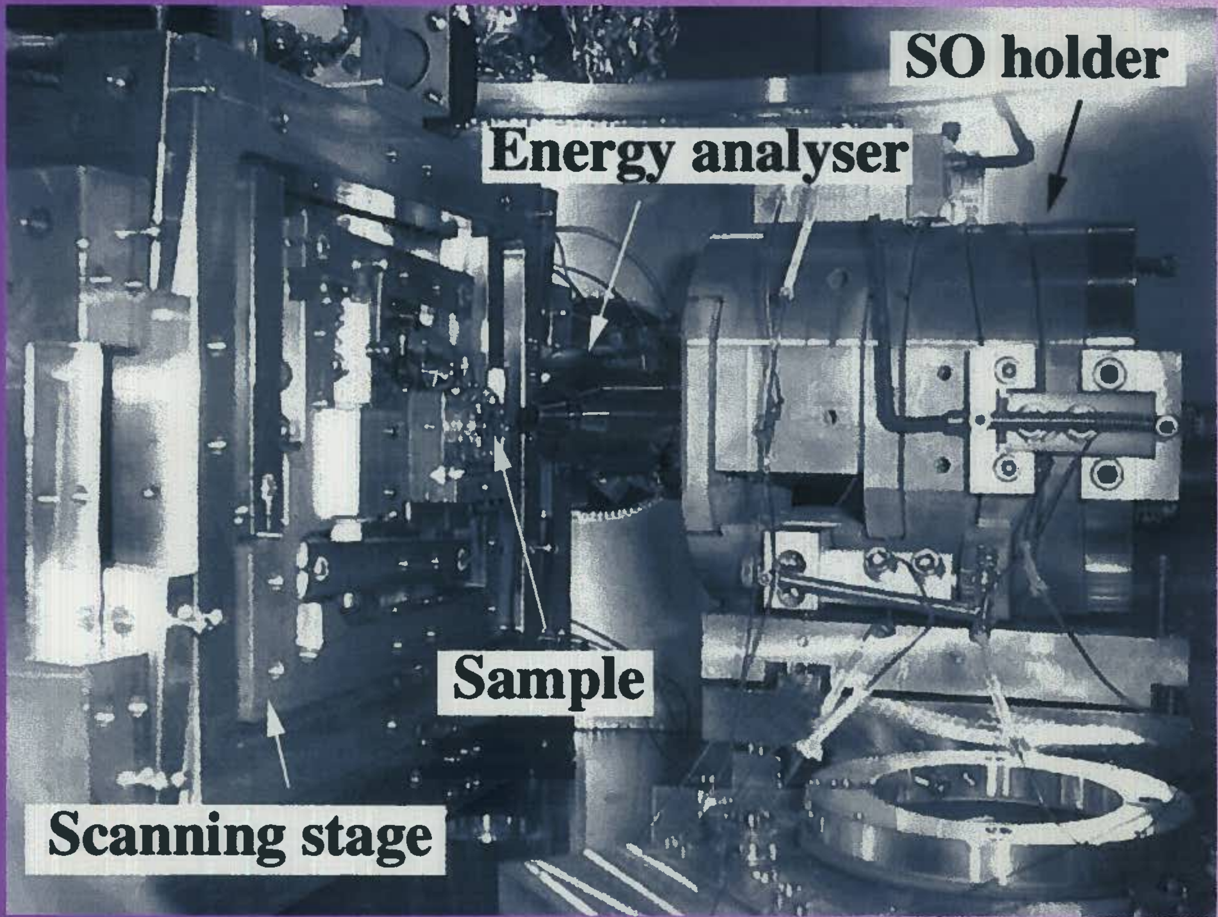

← light

Photon Energies:
74 eV (Mo/Si)
95 eV (Mo/Si)
110 eV (Ru/B_4C)

Spatial Resolution:
0.5 µm

Energy Resolution:
100 meV

F. Barbo, M. Bertolo, A. Bianco, G. Cautero, S. Fontana, T. K. Johal, S. La Rosa, G. Margaritondo, and K. Kaznacheyev, Rev. Sci. Instrum. 71 (2000) 5.

Objective Yield

S.O. yield = intensity after S.O. / intensity before S.O.

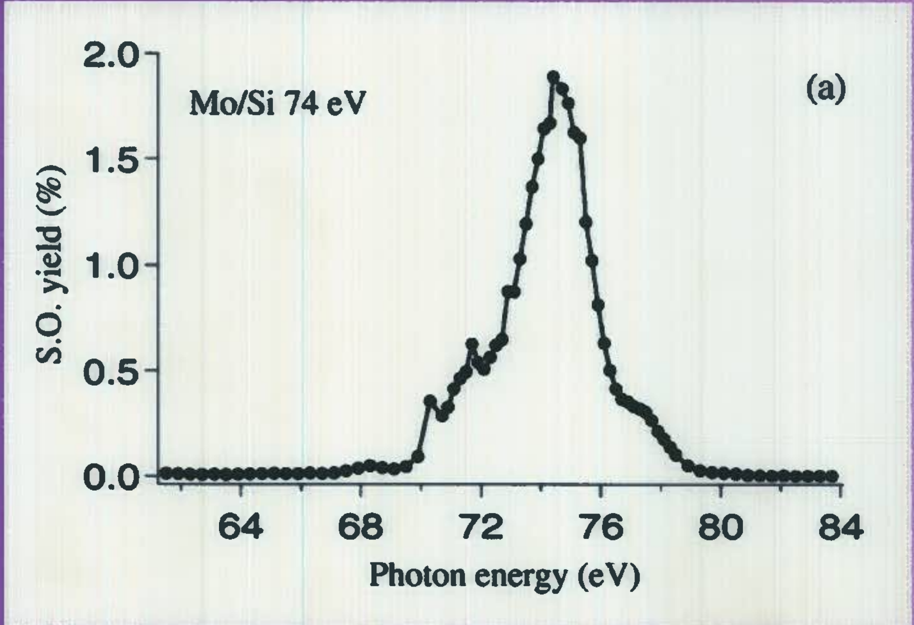

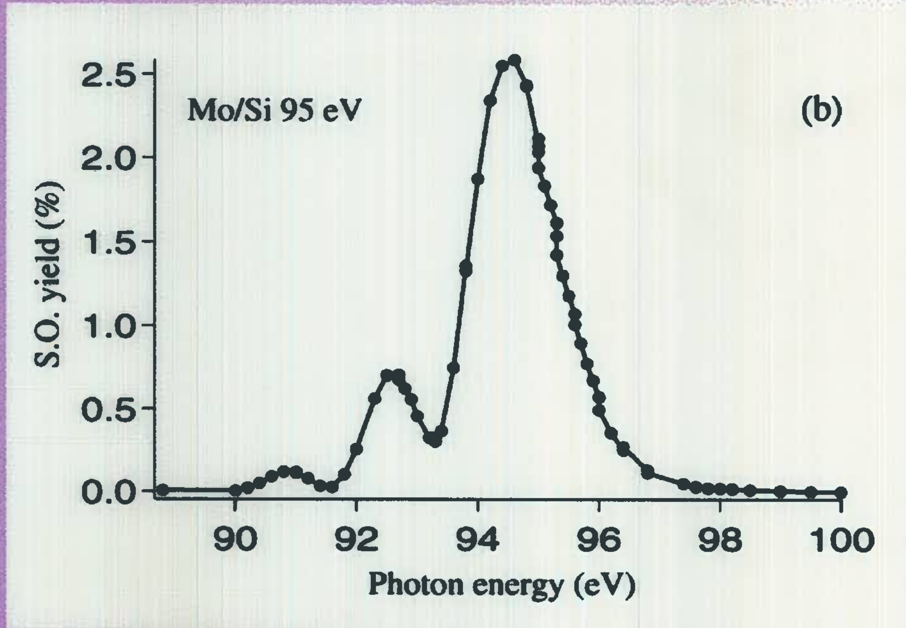

F. Barbo, M. Bertolo, A. Bianco, G. Cautero, S. Fontana, T. K. Johal, S. La Rosa, G. Margaritondo, and K. Kaznacheyev, Rev. Sci. Instrum. 71 (2000) 5.

Lateral Resolution

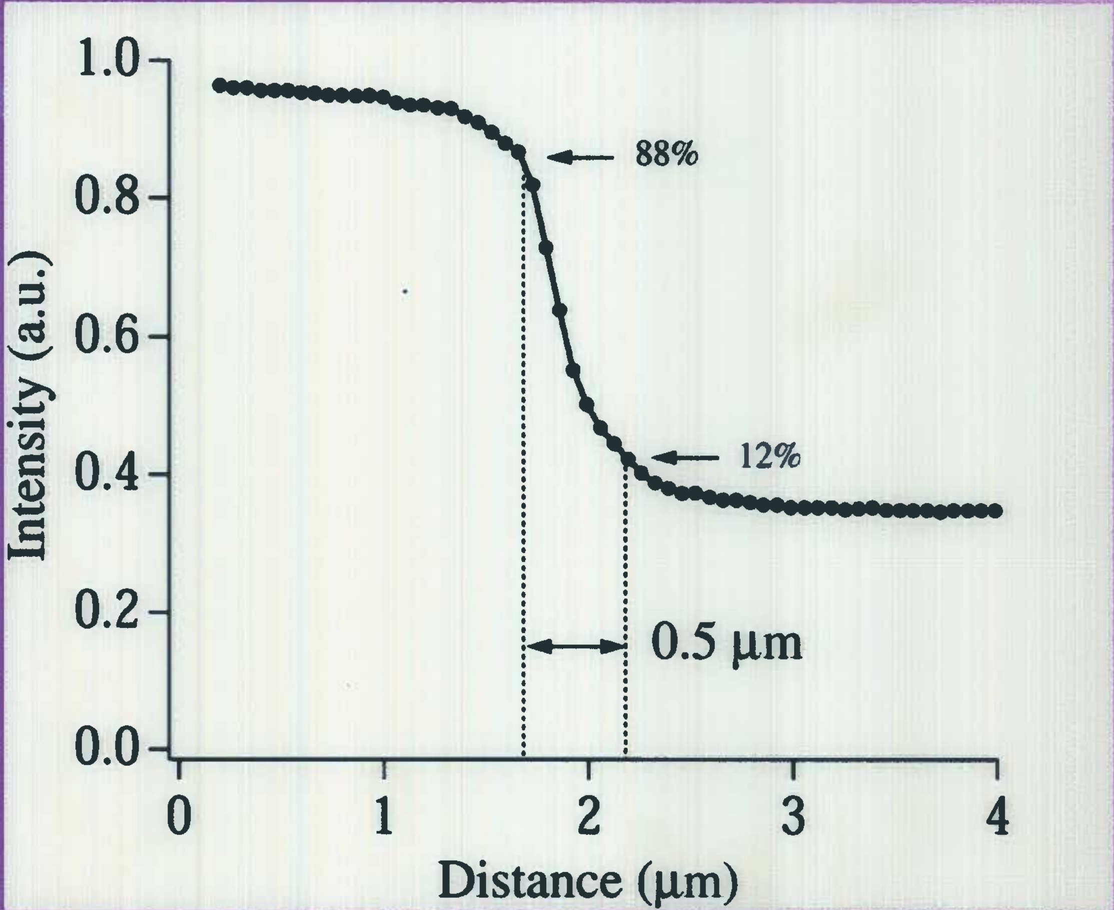

obtained by scanning knife edge across focus

Lateral resolution: 0.5 µm

Limited by abberations due to mirror's slope error

~ better mirrors
2001 : 0.1µm

F. Barbo, M. Bertolo, A. Bianco, G. Cautero, S. Fontana, T. K. Johal, S. La Rosa, G. Margaritondo, and K. Kaznacheyev, Rev. Sci. Instrum. 71 (2000) 5.

Diffuse Photon Background

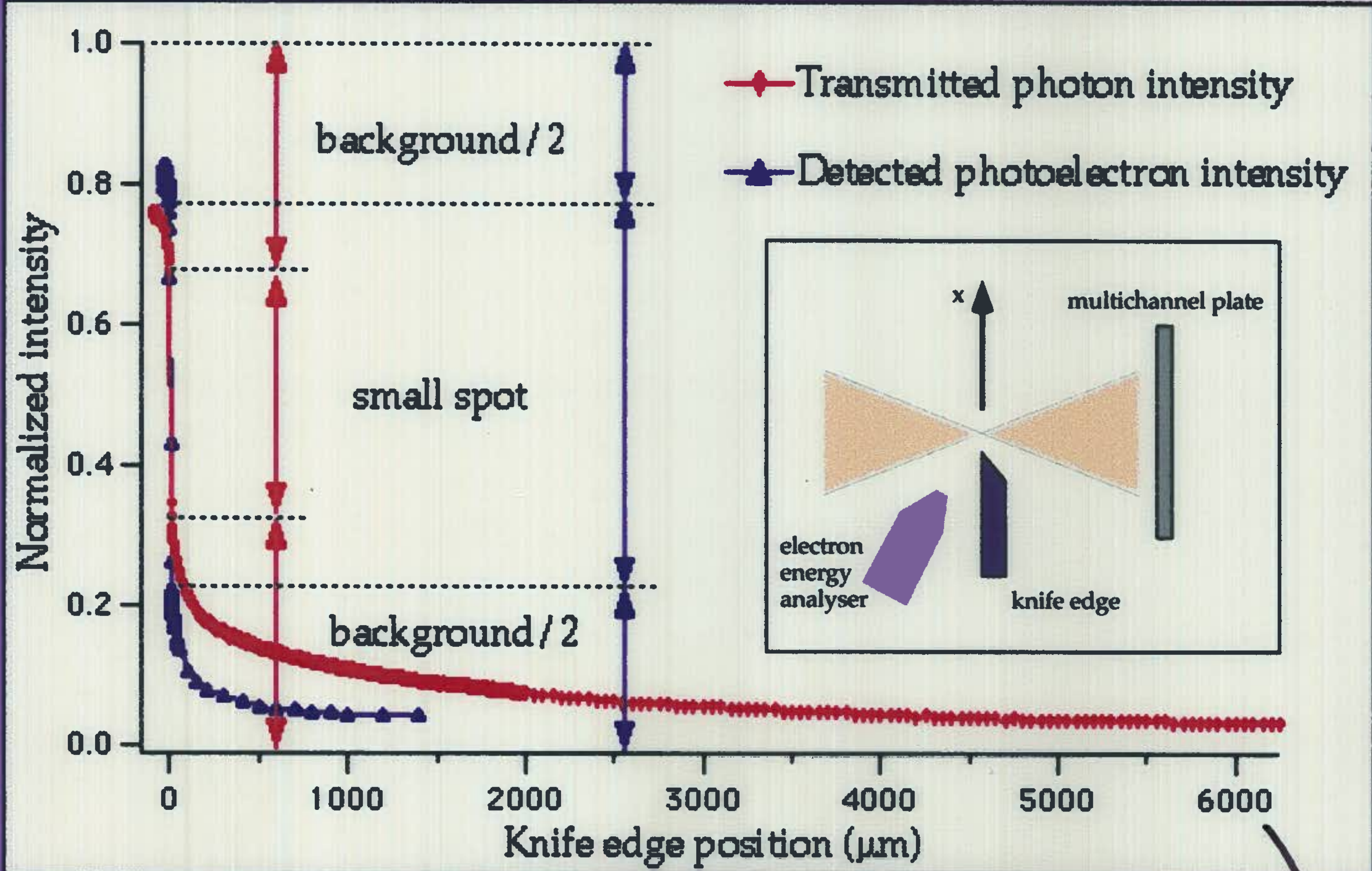

6mm!

In the spot:
35% photons
55% photoelectrons detected

In the background:
65% photons
45% photoelectrons detected

→ operate analyzer in small area detection mode

Ø 100μm: b.g. signal < 5%

F. Barbo, M. Bertolo, A. Bianco, G. Cautero, S. Fontana, T. K. Johal, S. La Rosa, G. Margaritondo, and K. Kaznacheyev, Rev. Sci. Instrum. 71 (2000) 5.

Imaging Abilities

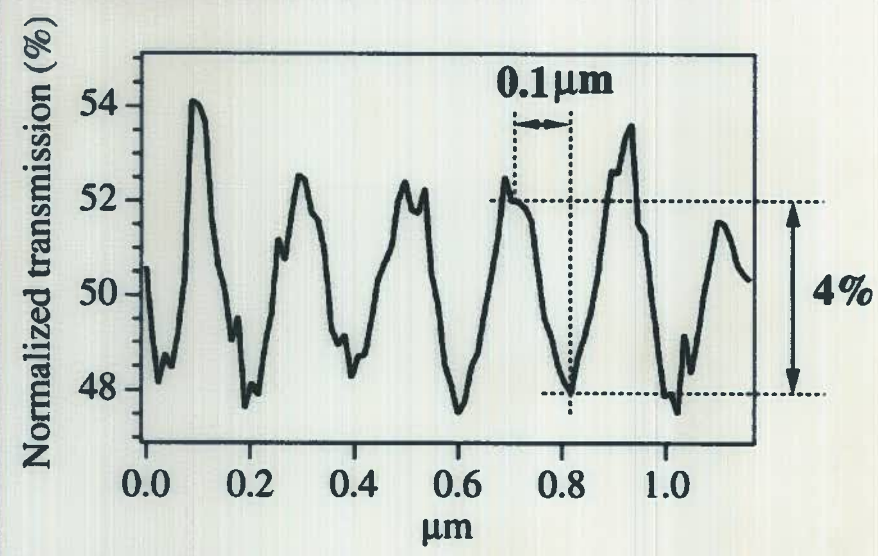

Features down to 0.1 µm can be resolved.

F. Barbo, M. Bertolo, A. Bianco, G. Cautero, S. Fontana, T. K. Johal, S. La Rosa, G. Margaritondo, and K. Kaznacheyev, Rev. Sci. Instrum. 71 (2000) 5.